Paper No.
7274

NACE INTERNATIONAL CORROSION 2016 CONFERENCE & EXPO

Role of Amine in the Mitigation of CO_2 TOP of the line Corrosion

Z. Belarbi
Institute for Corrosion and MultiphasTechnology
Ohio University
342 West State Street
Athens, OH 45701

F. Farelas
Institute for Corrosion and MultiphasTechnology
Ohio University
342 West State Street
Athens, OH 45701

M. Singer
Institute for Corrosion and MultiphasTechnology
Ohio University
342 West State Street
Athens, OH 45701

S. Nesic
Institute for Corrosion and MultiphasTechnology
Ohio University
342 West State Street
Athens, OH 45701

ABSTRACT

Top-of-the-line corrosion (TLC) has the potential to lead to rapid loss of pipeline integrity. TLC also presents unique challenges in relation to its mitigation. Amine compounds are traditionally used as corrosion inhibitors in packages for mitigating CO_2 corrosion of carbon steel. They are also claimed to be effective volatile corrosion inhibitors also the mechanism involved in less clear. The principal objective of this work is to investigate and understand the TLC inhibition mechanism in the presence of diethylamine (DEA) and morpholine. In order to determine possible interactions between the tested amines and the steel surface, the surface charge was investigated by determining the potential of zero charge (PZC). The PZC was measured by means of electrochemical impedance spectroscopy (EIS) in a 1 wt.% NaCl solution at different pH values. The possible inhibitive properties of DEA and morpholine were first tested at the bottom of the line conditions by linear polarization resistance (LPR) and EIS, followed by TLC tests. The weight loss method was used to measure the corrosion rate at the top-of-the-line. After the experiments, the steel surface was characterized by scanning electronic microscopy (SEM). The results were interpreted based on the surface charge and provided key information about the possible mechanisms of adsorption amines (DEA and morpholine) on the steel surface. Results showed that the effect of the selected amines on the corrosion rate could be directly linked to the change in solution pH, both at the top and bottom of the line. Considering that the amines were almost fully protonated in the range of pH tested, their vapor pressures and consequently their concentrations in the condensed water were also very low, limiting further their effect on the corrosion at the top of the line. In addition, DEA and morpholine did not seem to have significant filming properties.

Keywords*:* CO_2 corrosion, morpholine, PZC, volatile amine, inhibition

INTRODUCTION

Top of the Line Corrosion (TLC) is a phenomenon encountered in wet gas transportation when problems of corrosion appear inside the pipe due to the condensation of water vapor containing dissolved corrosive gases. One way to minimize TLC of carbon steel pipelines exposed to CO_2 environments is by the use of volatile corrosion inhibitors (VCIs). VCIs used in industry are often a complex mixture of several compounds, e.g. a mixture of imidazolines salts and light amines (triethylenetetramine, diethylamine, methoxypropylamine, pyridine salts) at particular ratios. [1, 2, 3] Therefore, it is important to understand how volatile amine compounds mitigate CO_2 corrosion. Morpholine has been used as a corrosion inhibitor and VCI for carbon steel exposed to alkaline conditions [4] and 2N H_2SO_4 and 2N H_3PO_4 solutions. [5] It has been shown that a better inhibition was obtained in 2N phosphoric acid. Diethylamine was tested in petroleum/water corrosive mixtures at 25°C [6] and has been used as corrosion inhibitor for carbon steel in aqueous solution at pH of 11.4. The results showed that the presence of Diethylamine induced the formation of a layer providing protective properties to the metal. [7] The level of adsorption of amines depends on their chemical structure, environment (acid or basic solution), metal surface condition and electrochemical potential at the interface. The adsorption process is governed by the charge on the metal surface and the chemical structure of the inhibitor. Physical adsorption is due to the electrostatic attraction between the inhibiting ions and the electrically charged surface of the metal which is defined by the position of the free corrosion potential with respect to its potential of zero charge (PZC). PZC is the potential where the metallic side of the double layer has no excess charge. It offers itself as a natural reference point to identify the surface charge. If the metal potential is greater than the potential of zero charge, the metal is said to be positively charged and the adsorption of anions is favored. Conversely, the adsorption of cations is preferred if the free corrosion potential is below PZC. [8]

Figure 1 and Figure 2 show the possible interactions between the steel surface, assuming that it is positively charged, and the protonated and non-protonated amine, respectively. In solutions with dissolved CO_2 (acidic solutions), amines quickly protonate due to their basicity. In a NaCl solution, Cl^- and water molecules absorb on the steel surface and interact with the protonated amine forming electrostatic bonds (). For the case of un-protonated amines, the nitrogen atom (heteroatom) poses a free electron pair which can form Van der Waals bonding with the steel surface, . In both cases, amines can easily desorb because they do not form a chemical bond. The formation of a donor-acceptor bond between the metal and inhibitor is not possible because the non-oxidized steel surface is not an electron acceptor. In order to form a donor-acceptor bond, the acceptor should have an open “box”, box diagram of outer electron orbitals for the electron configuration of atoms, available to accept two electrons. In the case of morpholine, oxygen cannot form Van der Waals bonding with the steel surface because it has a lower electron-donor capability than nitrogen. [9]
The objective of this paper is to investigate and understand the TLC inhibition mechanism in the presence of diethylamine (DEA) and morpholine and identify the type of chemical or physical bonds likely to form between the amines and the carbon steel surface.

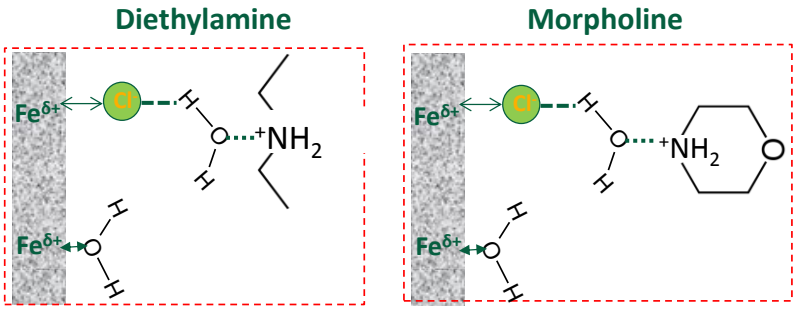

Figure 1: Possible interactions between protonated amine functional groups and metal surface. [8, 10] (⟺): Electrostatic interaction between induced dipole ($Fe^{\delta+}$) and anion (Cl^-). (- - -): Hydrogen bonding. (·····): Electrostatic interaction between permanent dipole (H_2O) and cation ($-NH_2^+$). (◄►): Van der Waals bonding.

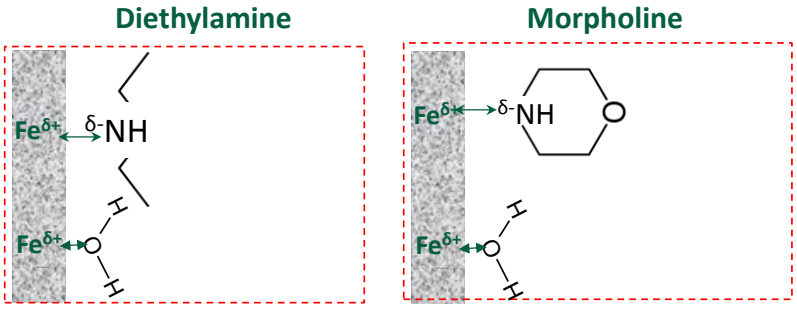

Figure 2: Possible interactions between non-protonated amine functional groups and metal surface. [8, 10] (⟷): Van der Waals bonding.

EXPERIMENTAL PROCEDURE

Materials and Chemicals

The amines (morpholine and diethylamine) used in this research were acquired from Sigma-Aldrich. Samples for electrochemical and weight loss measurements were made of API 5L X65 carbon steel. The chemical composition of the carbon steel is provided in Table 1.

Table 1
Composition (wt.%) of API[(1)] 5L X65 carbon steel

Element	C	Nb	Mn	P	S	Ti	V	Ni	Fe
X65	0.05	0.03	1.51	0.004	<0.001	0.01	0.04	0.04	balance

Electrochemical measurements (Bottom of the line tests)

An electrochemical cell with a three-electrode set up was used (Figure 3). A carbon steel X65 rotating cylinder electrode (RCE), a platinum grid, and $Ag/AgCl_{sat}$ electrode were used as working, counter, and reference electrodes, respectively. The reference electrode was placed in a separate cell and was connected to the corrosion cell *via* a salt bridge and a Luggin capillary. The RCE was ground with silicon carbide paper (600 grit), cleaned with isopropanol

(1) American Petroleum Institute (API), 1220 L St. NW, Washington, DC 20005.

in an ultrasonic bath and air-dried before introduction in the cell. The experiments were performed in deionized water containing 1 wt. % NaCl at 25°C. The solution was deoxygenated for 2 hours with CO_2 prior to the introduction of the working electrode. To avoid the noise caused by CO_2 bubbling, the sparge tube was pulled up to the headspace during the entire experiment. CO_2 was purged continuously throughout the experiment in order to avoid oxygen contamination and to maintain saturation with CO_2 of the test solution. A pH probe was used to measure the pH of the solution before and after adding the respective amine. The rotation speed of the working electrode was set at 1000 rpm before starting any electrochemical measurement.

The Potential of Zero Charge (PZC) was identified by means of electrochemical impedance spectroscopy (EIS) at different pHs. Prior to any measurement, the open circuit potential (OCP) was monitored during 8 minutes to ensure a stable potential value ($\Delta E < 5$ mV). Impedance was sampled in the frequency range of 10 kHz-0.1 Hz taking 7 points per decade. The amplitude of the *ac* signal was 10 mV (rms) from the OCP. Corrosion rate was assessed by linear polarization resistance (LPR) and EIS Measurements were taken every 40 minutes during an exposure time of 14 hours. All measurements were performed with a potentiostat/galvanostat instrument (Gamry®[(2)]).

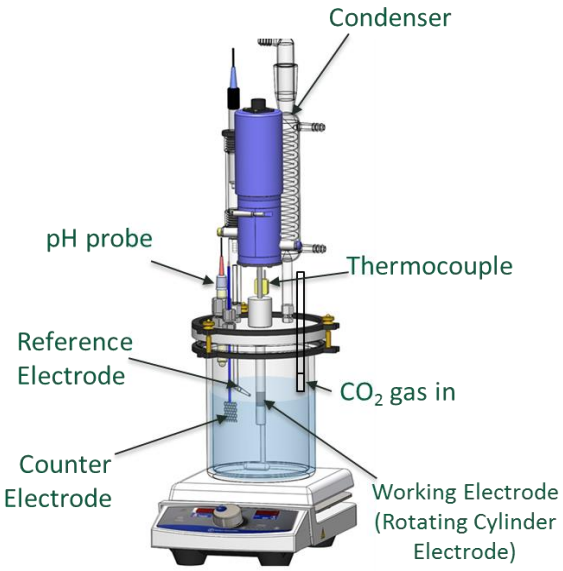

Figure 3: Experimental setup for electrochemical tests (BLC).

Weight loss measurements (TLC tests)

The experimental setup used for evaluating the efficacy of VCIs under TLC conditions is shown in Figure 4. Since it is difficult to perform electrochemical measurements on samples exposed to TLC conditions, the weight loss technique was used to measure the corrosion rate at the top of the line. The bulk aqueous phase was comprised of deionized water containing 1wt.% NaCl, purged with CO_2 for 2 hours. Carbon steel X65 samples (exposed area = 7.917 cm^2) were prepared following the procedure described in the previous section. A pH probe was used to measure the pH at the bottom solution before and after adding the VCI. In order to have a gas temperature of 65°C, the bottom solution was heated to 72°C. A weight loss specimen was flush-mounted at the top of the experimental setup, controlling its temperature

[(2)] Potentiostat manufacturer of electrochemical Instruments

at 32°C using a cooling coil. Corrosion rate of the specimen at the top (TLC rate) with and without the addition of inhibitors was measured following the ASTM[3] G1 standard. [11] Consequently, measurements of TLC rates were performed in the condensed water phase, containing dissolved CO_2 and inhibitor.
The average corrosion rate can be determined by:

$$CR = (K * W)/(A * t * \rho) \qquad (1)$$

where:
CR: Corrosion rate in mm/y
K: Conversion factor 1.14×10^{-5}
W: Mass loss in grams,
A: Area in cm^2,
t: Time of exposure in hours,
ρ: Density of steel 7.87 g/cm^3.

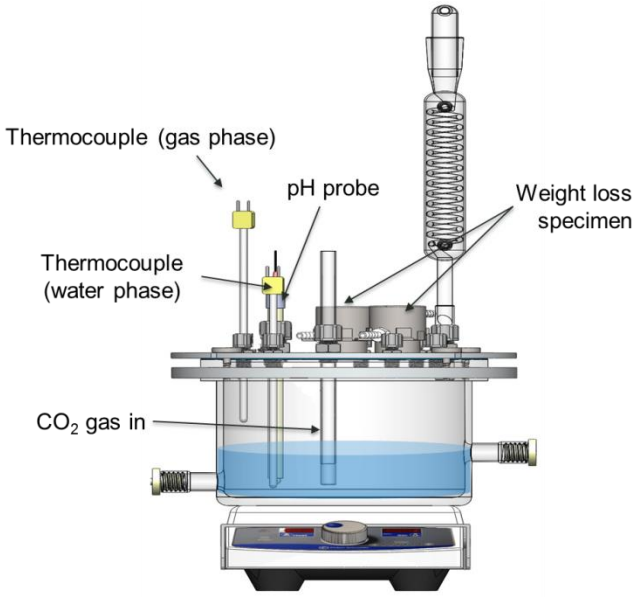

Figure 4: Experimental setup for evaluating efficacy of VCI candidates for TLC.

Surface analysis

Surface analysis of the exposed electrode was investigated by means of a Joel JSM-6090 LV scanning electron microscope. Imaging was performed at an accelerating voltage of 15 kV using secondary electron detector (SEI).

RESULTS AND DISCUSSION

Identification of steel surface charge

The potential of zero charge (PZC) is directly related to the surface work function, and its value is determined by the presence of a net dipole moment along the surface normal. [12] The work function, a fundamental electronic property of a metallic surface, is extremely sensitive to surface conditions (e.g. pH, impurities), pH being the most important factor that affects the

[3] American Society for Testing and Materials *(*ASTM*), 100 Barr Harbor Drive, West Conshohocken, PA, 19428-2959.*

PZC. Taking into account the previous statement, experiments were performed at pH values of 3.84, 5.15 and 5.30 in order to conduct theoretical calculations. This pHs are typical values measured in condensed water. According to Lorenz *et al.* [13], the potential of zero charge can be determined from EIS measurements through the calculation of the double layer capacitance, C_{dl}. In this research, EIS measurements were recorded at different potentials from the OCP, on a bare electrode, in the frequency range of 10 kHz to 0.1 Hz taking 7 points per decade. It follows from Figure 5 (pH 5.3) that a high frequency (HF) depressed charge-transfer semicircle was observed which is characteristic of distributed values of $C_{dl,}$ (constant phase element (CPE)). The same behavior was seen at pH 5.15 and 3.84 (not shown in this manuscript). To justify the existence of the CPE, the logarithm of the imaginary part of the impedance was plotted with respect to the logarithm of the frequency in the HF domain (Figure 6).The CPE impedance is defined as follows [14]:

$$Z_{CPE} = \frac{1}{Q_{eff}(j\omega)^{\alpha}} \qquad (2)$$

where $0 < \alpha < 1$ and Q_{eff} is the effective high-frequency capacity. Note that for a value of $\alpha = 1$, the Q_{dl} value directly corresponds to C_{dl}. The value of the slope of the red line shown in Figure 6, which provided a coefficient $\alpha = 0.74$ at -0.7 V *vs.* $Ag/AgCl_{sat}$ and pH 5.3, confirms the presence of the CPE in the HF domain. The graphical method was used to identify the CPE parameters (Q_{dl} and α) [14]. This method is the first step toward interpretation and evaluation of impedance data, and does not depend on any specific equivalent circuit model.

Q_{eff} or the CPE coefficient, when $\alpha \neq 1$, can be obtained directly from the imaginary part of the impedance as:

$$Q_{eff} = -\sin\left(\frac{\alpha\pi}{2}\right)\frac{1}{(2\pi f)^{\alpha} Im\ Part} \qquad (3)$$

when $\alpha = 1$, the CPE coefficient Q_{eff} becomes a capacitance, and equation (4) can be written as:

$$Q_{eff} = C_{dl} = \frac{-1}{(2\pi f) Im\ Part} \qquad (4)$$

The effective CPE coefficient is given in Figure 7. The high-frequency asymptote provides the value for the double-layer CPE coefficient. It is important to point out that the assessment should be made at frequencies significantly larger than the largest characteristic relaxation frequency for the system.

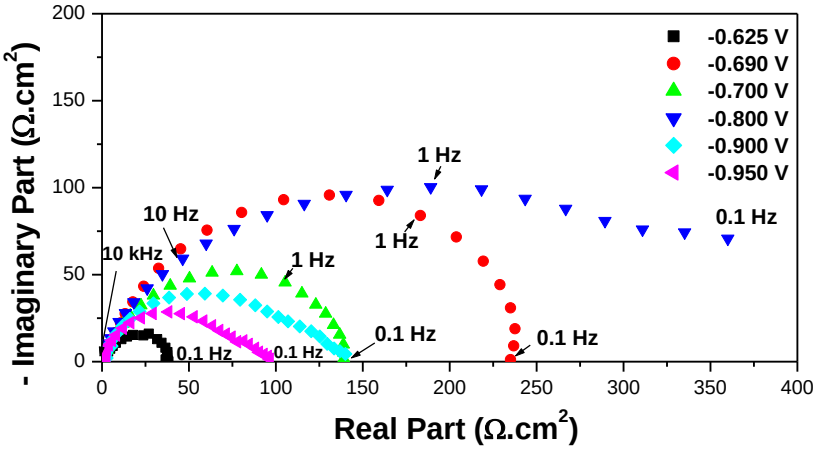

Figure 5: Nyquist plot of carbon steel in 1 wt.% NaCl solution at 25°C as a function of potential. pH = 5.3

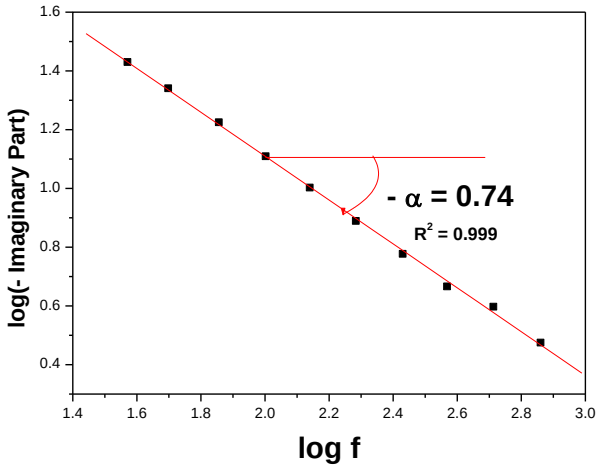

Figure 6: Representation of the logarithm of the imaginary part of the impedance vs. the logarithm of the frequency at the potential of -0.7V *vs*. Ag/AgCl and pH 5.3. The slope of the red line leads the *α* coefficient in Equation (2) to be obtained

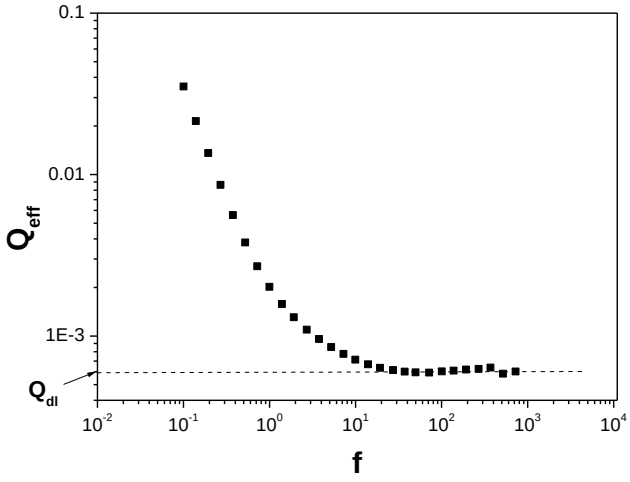

Figure 7: Effective CPE coefficient defined by equation (3) as a function of frequency at -0.7 V *vs*. Ag/AgCl and pH 5.3

Brug *et al*. [15] equation is used to calculate the value of C_{dl} in function of *R*s, Q_{dl} and *α*:

$$C_{dl} = R_s^{\frac{(1-\alpha)}{\alpha}} Q_{dl}^{\frac{1}{\alpha}} \qquad (5)$$

The solution resistance (R_s), is given by the intersection of the high frequency impedance with real axis in the Nyquist plot (Figure 5). EIS measurements at different potential and pHs were used to calculate the capacitance of double layer, C_{dl}. Figure 8 represents the C_{dl} values calculated from Equation (5) with respect to the applied potential, E, at different pHs. The minimum value on the C_{dl} versus *E* curve represents the PZC of the electrode. The values of PZC at the selected pHs are shown in Table 2. As it can be seen, the values of PZC obtained at pH 5.15 and 5.3 are more negative than that the observed at pH 3.84. Such an effect may be due to the change of the species concentration in solutions (H^+ ion in acidic solutions). [16] PZC is dependent on the work function and it is seen to be an important electrochemical propriety of the metal. The work function in the metal is equal to ionization energy (minimum energy to remove an electron from an atom) and it is strongly affected by the condition of the surface (e.g. the surface is different in acid, basic or neutral solutions). [17]

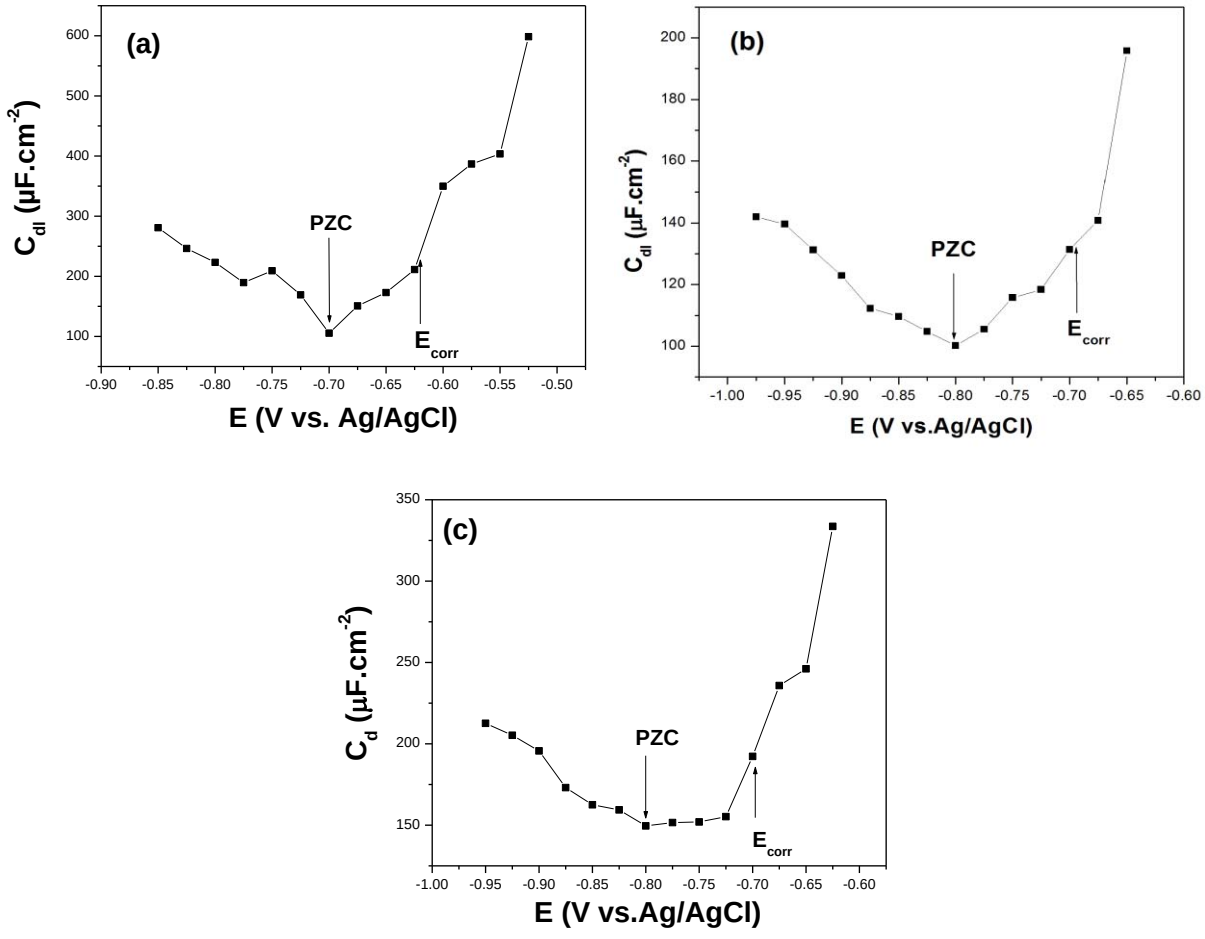

Figure 8: C_{dl} value calculated from Equation (5) values with respect to applied potential at different pH. a). pH = 3.84. b). pH = 5.15. c). pH = 5.3.

Table 2
Values of the PZC and (OCP−PZC) recorded for steel electrode in 1wt.% NaCl solutions in the pH range (3.84–5.3) at 25 ◦C

	pH 3.84	**pH 5.15**	**pH 5.3**
PZC (V *vs.* Ag/AgCl)	-0.7	-0.8	-0.8
OCP (V *vs.* Ag/AgCl)	-0.62	-0.68	-0.69
OCP- PZC (V)	0.08	0.12	0.11

Comparing the values of the PZC obtained in the pH range of 3.84 to 5.3 with the corresponding OCP values, it is possible to deduce that the steel surface is positively charged at the conditions of the present study (see the positive values of the difference OCP- PZC in Table 2). These results confirm the electrostatic adsorption of amines, previously shown in Figure 1 and Figure 2 on a positively charged steel surface exposed to NaCl solutions in this pH range.

BLC testing

In order to study the inhibition propriety of the selected amines, the tests were performed first in the water phase followed by experiments in the vapor phase. The results of testing morpholine are shown in Figure 9. All the measurements were performed at room temperature (25 °C). The corrosion rate and pH were measured before and after the addition of the amine (Table 3). In the absence of amine, corrosion rate and OCP are equal to 2.8 mm/y and -0.64 V vs. Ag/AgCl, respectively. In the presence of morpholine corrosion rate **(**CR ≈ 1.91 mm/y) did not significantly change as compared to the uninhibited condition (CR ≈ 2.8 mm/y). OCP decreased to become more negative. Such an effect may be due to the decrease of species reduction at the steel surface (change of H^+ ion in acidic solutions).

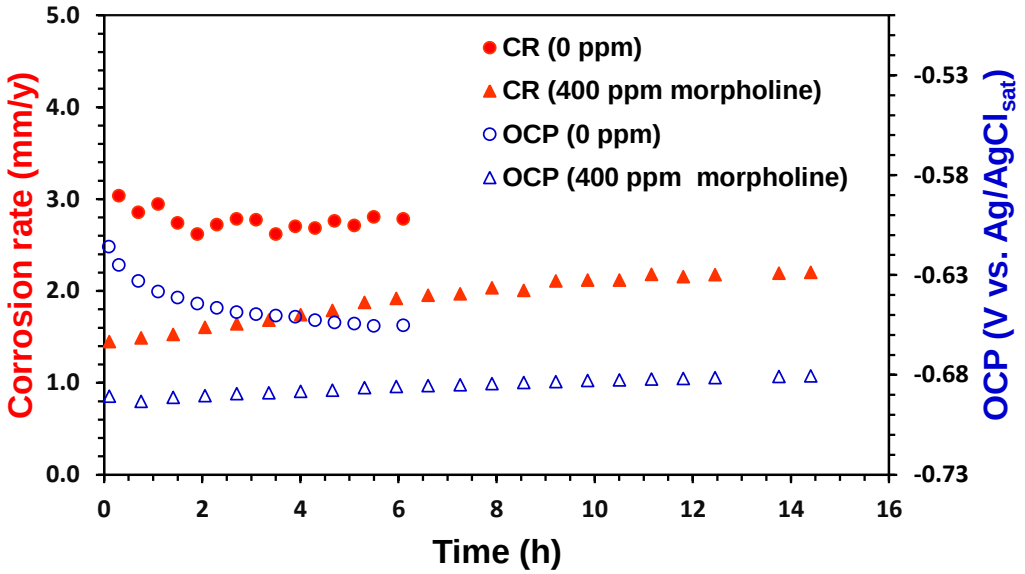

Figure 9: OCP and BLC rate of X65 rotating cylinder electrode in 1 wt.% NaCl solution at 25°C as a function of time. The red lines are the BLC rates, and the blue lines are OCP. Circular points are for the uninhibited specimen and the triangular points are for the specimens inhibited by 400 ppm_V morpholine.

Figure 10 shows the impedance diagrams in the Nyquist plane versus time. The Nyquist plot of the inhibited electrode is characterized by depressed semicircles at high to medium frequencies and inductive loops at low frequencies. The high frequencies semicircle is attributed to the time constant of charge transfer and double layer capacitance. The inductive loop may be attributed to the relaxation process obtained by adsorption species as Cl_{ads}^{-} and H_{ads}^{+} on the electrode surface. The presence of morpholine increases the impedance but does not change other aspects of the behavior. The charge transfer resistance, R_t, is given by the intersection of the low frequency end of the Nyquist plot with the abscissa. R_t was used to calculate corrosion rate. Figure 11 shows a good agreement between CR measured by LPR and EIS. The same behavior is observed in the presence of diethylamine (Figure 12).

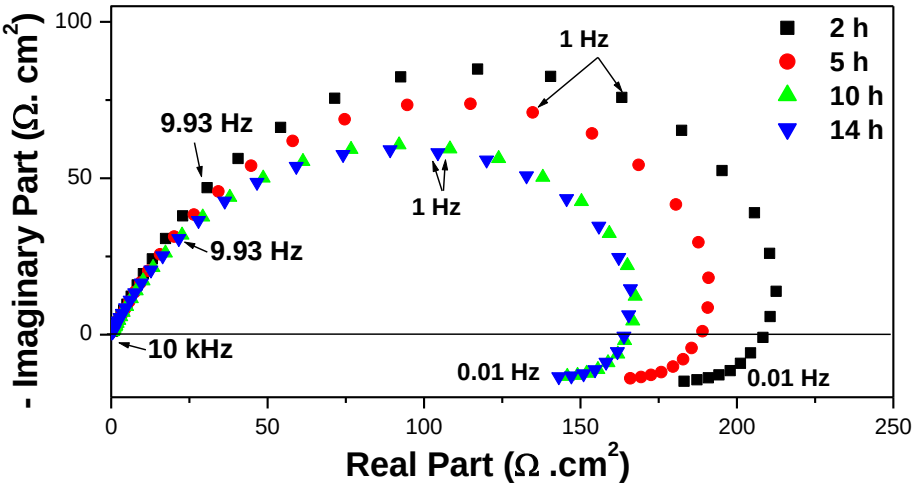

Figure 10: The Nyquist plot of carbon steel in in 1 wt.% NaCl solution at 25°C as a function of time in the presence of morpholine.

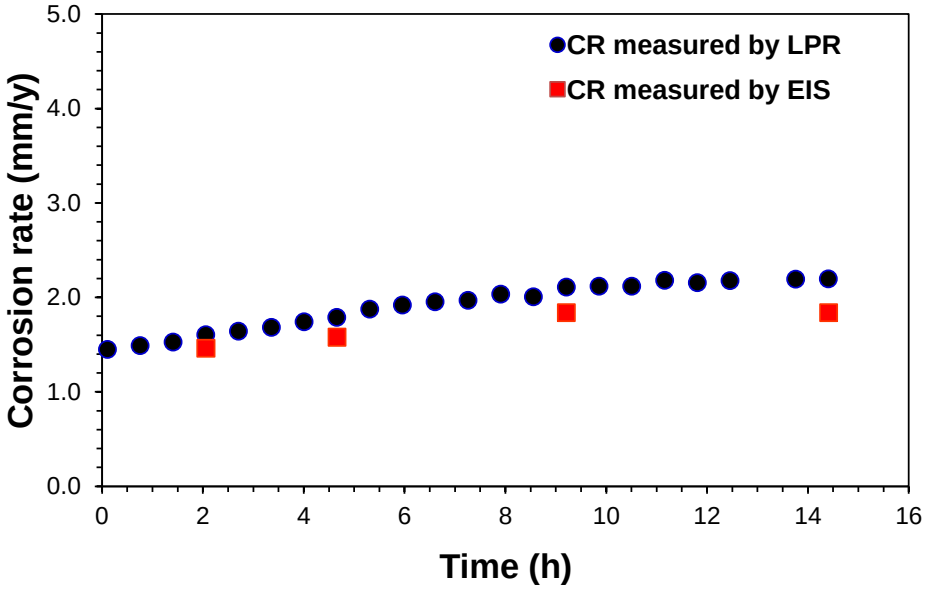

Figure 11: Comparison between CR measured by LPR and CR measured by EIS in the presence of morpholine.

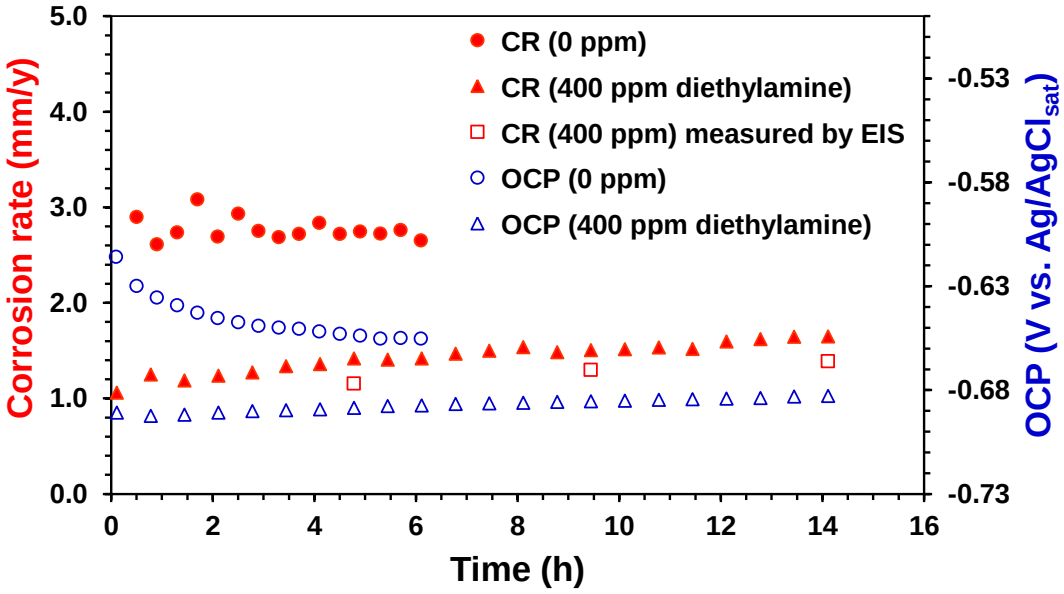

Figure 12: OCP and BLC rate of X65 rotating cylinder electrode in 1 wt.% NaCl solution at 25°C as a function of time. The red lines are the BLC rates, and the blue lines are OCP. Circular points are for the uninhibited specimen and the triangular points are for the specimens inhibited by 400 ppm_V diethylamine.

In the light of these measurements, morpholine and diethylamine have shown poor inhibition in an acid environment. In order to clarify if the decrease of corrosion rate after the addition of the respective amine was due to the increase of pH or by the adsorption on the steel surface, a comparison between the measured corrosion rate and calculated corrosion rate (using the Multicorp[4] was performed, shown Table 3. The corrosion rates after the addition of the tested amine are similar to the calculated corrosion rate without the addition of the amines at the same pH. Therefore, the decrease of corrosion rate could be ascribed to the increase of pH and not to adsorption of the neutral amines. It is understandable because these amines were easily protonated in the acid solution, the ratio of $[Amine]/[AmineH^+] \approx 10^{-8.5}$ and 10^{-11} for morpholine and diethylamine, respectively.

Table 3
Comparison measured corrosion rate and calculated corrosion rate due to pH change

Chemicals	Measured pH	Measured CR (mm/y)	Calculated CR using Multicorp (mm/y)	Measured CR without adding amine at the same pH (mm/y
Blank	3.79	2.8	4.6	-
Morpholine	5.26	1.9	1.6	1.85
Diethylamine	5.12	1.4	1.6	-

TLC testing

The TLC rate obtained by WL and surface images taken after the tests are shown in Figure 13 and Figure 14, respectively. The results show that under the baseline conditions, the X65

[4] Software developed by Institute for corrosion and multiphase technology, Ohio University

specimen was corroded at a TLC rate of 0.92 mm/y and its surface was fully covered by a corrosion product. In the presence of diethylamine and morpholine, the corrosion rate at the top decreased to 0.65 and 0.5 mm/y, respectively. Morpholine and diethylamine were not totally protonated in the bottom solution. Therefore, the neutral amine could evaporate causing a change in the pH of condensed water, decreasing the corrosion rate. It was explained in the previous section that amines do not form an adsorbed layer due to the positively charge steel surface. The same behavior should be expected at the top of the line, however in the condensed water there are no chloride ions, therefore the likelihood of neutral amine adsorption is low. The results show that morpholine and diethylamine did not fully protect the steel specimen exposed to the TLC conditions. The SEM images of this specimen surface (Figure 15, Figure 16 and Figure 17) confirmed this conclusion, showing alternating corroded and protected areas. EDS of the corroded surface shows the presences of alloying elements typical of a Fe_3C layer.

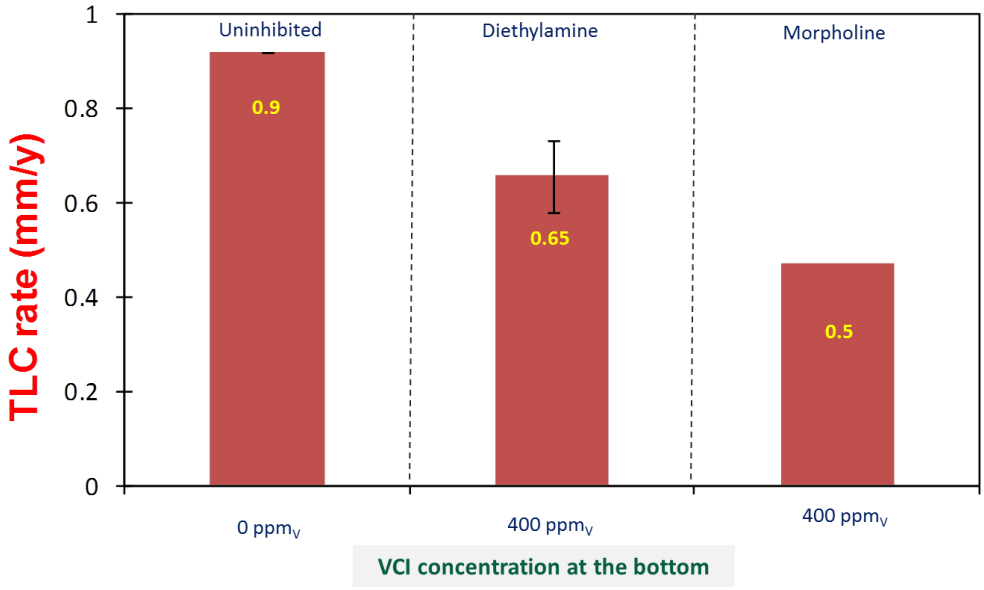

Figure 13: Corrosion rate by weight loss measurement of the uninhibited and inhibited TLC specimens (WCR = 0.6 mL/m^2/s). Note: VCI candidate concentrations on x-axes are the injected concentration for the bottom solution.

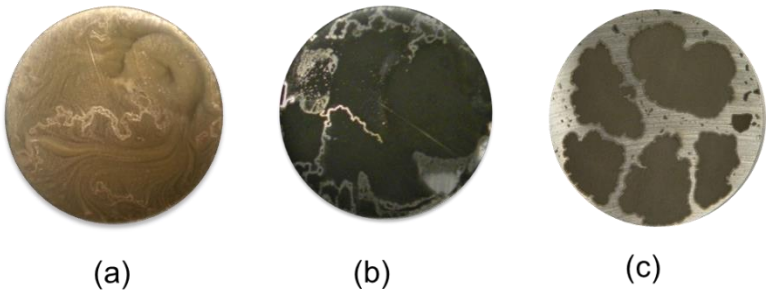

Figure 14: Visual images of sample exposed to corrosion in the co-condensation of water (WCR = 0.6 mL/m^2/s) in the presence of a) no inhibitor; b) 400 ppm$_V$ diethylamine; c) 400 ppm$_V$ morpholine after 2 days.

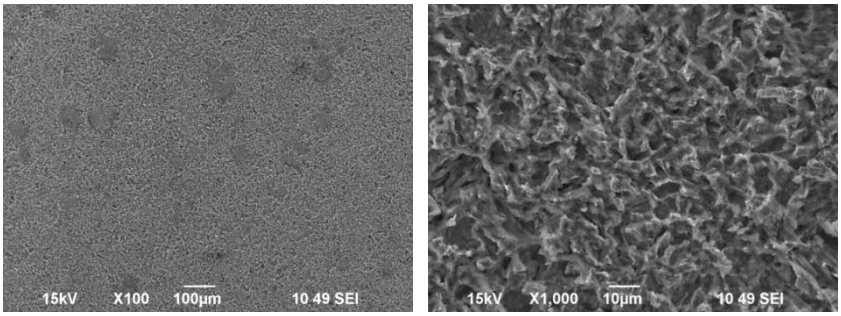

Figure 15: SEM images at different magnifications of the blank sample after 2 days.

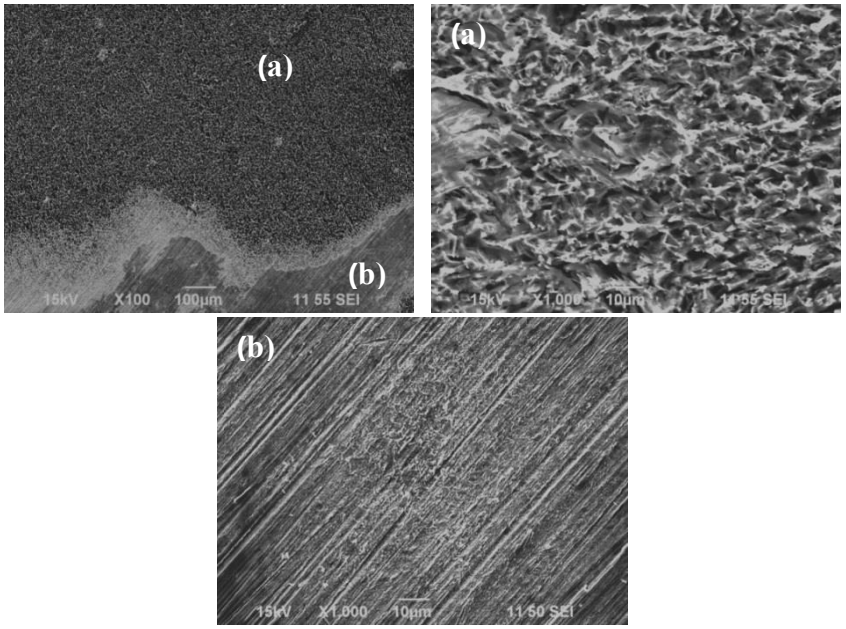

Figure 16: SEM images at different magnifications and locations (a: corroded surface; b protected surface) of the sample in the presence of 400 ppm of morpholine after 2 days.

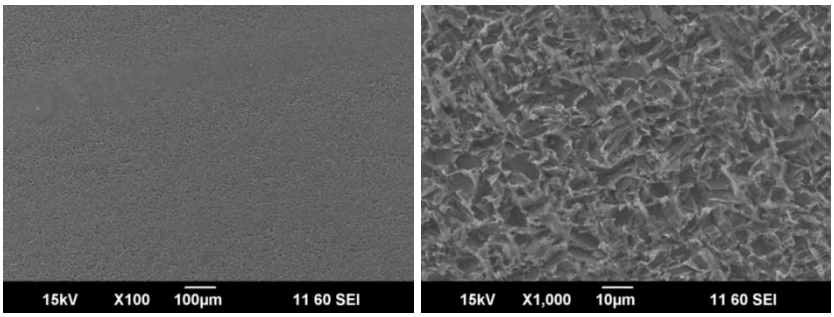

Figure 17: SEM images at different magnifications of the sample surfaces in the presence of 400 ppm of diethylamine after 2 days.

CONCLUSIONS

In this work, electrochemical techniques (electrochemical impedance spectroscopy and linear polarization resistance) and the weight loss method were used to study the TLC inhibition mechanism in the presence of diethylamine and morpholine in a CO_2 environment and acidic

pHs. The mechanisms were investigated by studying their interaction with the steel surface. As a result of this study, the following conclusions were drawn:

- Based on potential of zero charge measurements, it was found that the steel surface is positively charged; therefore the adsorption of anions (Cl^-) or permanent dipole is considered.
- The type of bonding and related interaction between amines and steel surface were identified by knowing the steel surface charge.
- The decrease of corrosion rate in the presence of morpholine and diethylamine could be attributed to the increase of pH after their addition in solution.
- Morpholine and diethylamine were protonated in acidic solutions and did not have significant filming properties due to the positively charge steel surface.
- If sufficient amount of amine is present in the condensed water, formation of $FeCO_3$ is favored due to an increase of pH.

ACKNOWLEDGMENTS

The author would like to thank the following companies for their financial support: Apache, BHP Billiton, BP, Chevron, ConocoPhillips, MI-SWACO, PETRONAS, PTTEP, Woodside and Talisman.

BIBLIOGRAPHY

[1] R.L.Matin, "Inhibtion of Vapor Phase Corrosion in Gas Pipetines," in *Corrosion/97, NACE*, Houston, 1997.

[2] R.L.Martin, "Inhibition of hydrogen permeation in steels corroding in sour fluids," *Corrosion,* vol. 49, no. 8, pp. 694-701, 1993.

[3] R.L.Martin, "Control of top-of-line corrosion in a sour gas gathering pipeline with corrosion inhibitors," in *NACE*, Houston, 2009.

[4] S.Nasrazadani, J. Diaz, J. Stevens and R. Theimer, "Effects of DBU, morpholine, and DMA on corrosion of low carbon steel exposed to steam," *Corrosion science,* vol. 49, pp. 3024-3039, 2007.

[5] K. Jayanthi, M. Sivaraju and K. Kannan, "Inhibiting properties of morpholine as corrosion Inhibitor for mild steel in 2N sulphuric acid and Phosphoric acid medium," *E-Journal of Chemistry,* vol. 9, no. 4, pp. 2213-2225, 2012.

[6] H. Ashassi-Sorkhabi and S. A. Nabavi-Amri, "Corrosion inhibition of carbon steel in petroleum /water mixtures by n-containing compounds," *Acta Chimica Slovenica,* vol. 47, pp. 507-517, 2000.

[7] V. Garcia-Arriaga, J. Alvarez-Ramirez, M. Amaya and E. Sosa, "H_2S and O_2 influence on the corrosion of carbon steel immersed in a solution containing 3 M diethanolamine," *Corrosion Science,* vol. 52, pp. 2268-2279, 2010.

[8] E.McCafferty, Introduction to corrosion science, Springer, 2010.

[9] A.Subramanian, M.Natesan, V. Muralidharan, K. Balakrishnan and T.Vasudevan, "An Overview: Vapor Phase Corrosion Inhibitors," *Corrosion,* vol. 56, pp. 144-155, 2000.

[10] R. Sokoll, H. Hobert and I. Schmuck, "Thermal desorption and infrared studies of amines adsorbed on SiO2, Al2O3, Fe2O3, MgO, and CaO," *Journal of Catalysis,* vol. 121, pp. 153-164, 1990.

[11] "Standard practice for preparing cleaning and evaluating corrosion test specimens," *ASTM-G1,* pp. 15-21, 1999.

[12] P. Ramıirez, R. Andreul, A. Cuestal, C. J. Calzado and J. Calvente, "Determination of the Potential of Zero Charge of Au(111) Modified with Thiol Monolayers," *Anal. Chem.,* vol. 79, pp. 6473-6479, 2007.

[13] W. J. Lorenz and H. Fischer, "Zum potential des ladungsnullpunktes des eisens-I," *Electrochimica Acta ,* vol. 11, pp. 1597-1605, 1966.

[14] M. E. Orazem and B. Tribollet, Electrochemical impedance spectroscopy, New Jersey: John Wiley & Sons; Inc.; Hoboken;New Jersey, 2008.

[15] G. J. Brug, A. G. V. D. Eeden, M. Sluyters-Rehbach and J. H. Sluyters, "The analysis of electrode impedances complicated by the presence of a constant phase element," *Journal of Electroanalytical Chemistry,* vol. 176, pp. 275-295, 1984.

[16] M. A. Amin, S. S. A. El-Rehim, E. El-Sherbini and R. S. Bayoumi, "The inhibition of low carbon steel corrosion in hydrochloric acid solutions by succinic acid Part I. Weight loss, polarization, EIS, PZC, EDX and SEM studies," *Electrochimica Acta ,* vol. 52 , p. 3588–3600, 2007.

[17] M. Chelvayohan and C. H. B. Mee, "Work function measurements on (110), (100) and (111) surfaces of silver," *Journal of Physics C: Solid State Physics,* vol. 15 , pp. 2305-2312, 1982.